

LASER GYROSCOPES

PACS numbers: 06.30.Bp; 07.07.Df; 32.60.+i; 42.60.By
DOI: 10.1070/QE2015v045n06ABEH015538

Effect of external and internal magnetic fields on the bias stability in a Zeeman laser gyroscope

Yu.Yu. Kolbas, I.I. Savel'ev, N.I. Khokhlov

Abstract. **With the specific features of electronic systems of a Zeeman laser gyroscope taken into account, the basic physical mechanisms of the magnetic field effect on the bias stability and the factors giving rise to the internal magnetic fields are revealed. The hardware-based methods of reducing the effect of external and internal magnetic fields are considered, as well as the algorithmic methods for increasing the stability of the bias magnetic component by taking into account its reproducible temperature and time dependences. Typical experimental temperature and time dependences of the magnetic component of the Zeeman laser gyro bias are presented, and by their example the efficiency of the proposed methods for reducing the effect of magnetic fields is shown.**

Keywords: *laser gyroscope, Zeeman effect, zero bias, magnetic drift.*

1. Introduction

The magnetic component of the zero bias in a Zeeman laser gyroscope (ZLG) is the term used for the component, depending on the magnetic field in an active medium, which can be selected in the quasi-four-wave ZLG oscillation regime (polarisation switching regime [1]). The instability of the zero bias magnetic component (magnetic drift of the zero) leads to an error in the angular velocity measurement and, therefore, should be minimised.

A few papers are devoted to the study of the magnetic component of the ZLG bias and its effect on the total measurement error [1–6]. However, their authors considered the magnetic drift in ZLGs as given, without explaining the underlying physical phenomena, both in the process of changing the external temperature and due to the self-heating or mechanical shocks and vibrations. It was only found that the magnetic sensitivity, i.e., the change in the frequency difference between the counterpropagating waves under the action of the magnetic field, applied to a ring laser (RL), linearly decreases with increasing temperature [7]. No explanation was given to the large magnetic drift that sometimes occurs in ZLGs due to the self-heating, as well as to the hysteresis of the magnetic drift under the temperature variations, and no physically explainable algorithm for correcting such drift was proposed [8]. Since at present, even when the quasi-four-wave regime is used, the ZLG error is essentially limited by the magnetic drift, the search for the answers to these questions becomes particularly important.

This paper presents the results of studying the magnetic drift in ZLGs that, in our opinion, fill in the gap in the publications, devoted to both the physical origins of the ZLG magnetic drift and the methods of its reduction.

The appearance of the magnetic component in the zero bias is determined by the sensitivity of the ZLG sensor, the ring He–Ne laser with circular polarisation of waves, to the magnetic field [1]; therefore, the causes of the magnetic drift are instabilities of the magnetic fields inside and outside the ZLG, as well as the instability of the sensitivity to the magnetic field of the ZLG itself. Since the instability of the external magnetic fields is determined by the conditions of the gyro exploitation, the main attention in the paper is paid to the causes of the appearance and the instability of the internal magnetic fields, as well as to the causes of instability of the ZLG sensitivity to the magnetic field, including the consideration of the specific manifestation of the sensitivity instability, associated with the operation of the ZLG functional electronic systems, the so called dynamic drift.

2. Magnetic component of the ZLG zero bias

If a longitudinal magnetic field with the strength H is applied to the active medium of a ring helium–neon laser, then due to the Zeeman effect the emission line in the spectrum of the active atoms is split by $\mu = g\mu_B H$, where g is the Lande factor, and μ_B is the Bohr magneton. Due to the frequency pulling effect, the Zeeman splitting leads to the appearance of a frequency difference between the counterpropagating waves f, depending on H and the detuning of the cavity frequency ω from the frequency of the gain maximum ω_0 [9]. If the cavity is tuned to the gain maximum ($\omega = \omega_0$), then

$$f(0) = \Delta\nu_r \frac{\eta}{\eta_0} Z_r\left(\frac{-\mu + i\gamma_{ab}}{ku}\right), \quad (1)$$

where $\Delta\nu_r$ is the cavity bandwidth; η is the gain excess over the losses; $\eta_0 = \max Z_i(i\gamma_{ab}/ku)$; Z_r and Z_i are the real and imaginary parts of the dispersion function for the plasma of gas discharge in the He–Ne laser, respectively; γ_{ab} is the homogeneous broadening parameter of the a→b transition line; k is the wave number; and u is the mean thermal velocity of atoms.

The cavity bandwidth is related to its losses as

$$\Delta\nu_r = (c/L)p,$$

Yu.Yu. Kolbas, I.I. Savel'ev, N.I. Khokhlov OJSC 'M.F. Stel'makh Polyus Research Institute', ul. Vvedenskogo 3, 117342 Moscow, Russia; e-mail: i.saveliev@gmail.com

Received 18 April 2014
Kvantovaya Elektronika **45** (6) 573–581 (2015)
Translated by V.L. Derbov

where c is the velocity of light; L is the cavity length; and p is the losses per roundtrip. The gain excess over the losses is expressed as

$$\eta = G/p,$$

where G is the gain per cavity roundtrip.

The dependence of the frequency difference f on the cavity detuning in the first approximation appears to be quadratic:

$$f(\omega - \omega_0) = f(0)\left[1 - \chi\left(\frac{\omega - \omega_0}{ku}\right)^2\right], \quad (2)$$

where χ is a weakly changing coefficient, depending on η and other parameters of the laser.

The oscillation frequency detuning can be related to the relative detuning of the oscillation wavelength λ in parts of the wavelength $\Delta\lambda$, which is commonly used in practice:

$$\omega - \omega_0 = 2\pi(c/L)\Delta\lambda; \quad (3)$$

then

$$f(\Delta\lambda) = f(0)\,[1 - \chi_0(\Delta\lambda)^2], \quad (4)$$

where $\chi_0 = \chi(c\lambda/uL)^2$.

To extract the magnetic component of the zero bias it is necessary to multiply the half-difference of the f values for the positive and negative values of the magnetic field by the scale factor of the ZLG, providing the result in the units of angular velocity.

The typical experimental dependences of the zero bias magnetic component on the RL temperature of four different ZLG sensors are presented in Figs 1a–d. In each of them 9 realisations of one sensor are shown. Each realisation started from the switched-off state after the temperature stabilisation of the ZLG, which was provided by keeping the ZLG at the given temperature and monitoring the temperature of its housing. The external temperature in each realisation was constant (its values are indicated at the abscissa axis and are nearly correspondent to the first point of each realisation). For the external temperature +25 °C three realisations are shown (one recorded at the beginning of the test, the second one after the increased temperatures and the third after the decreased temperatures).

The analysis of the specific features of these dependences requires the knowledge of the construction and operation of a modern ZLG.

3. Construction of a ZLG and specific features of its operation

The external view and the structure schematic diagram of the ZLG of the MT type (OJSC 'M.F. Stel'makh Polyus Research

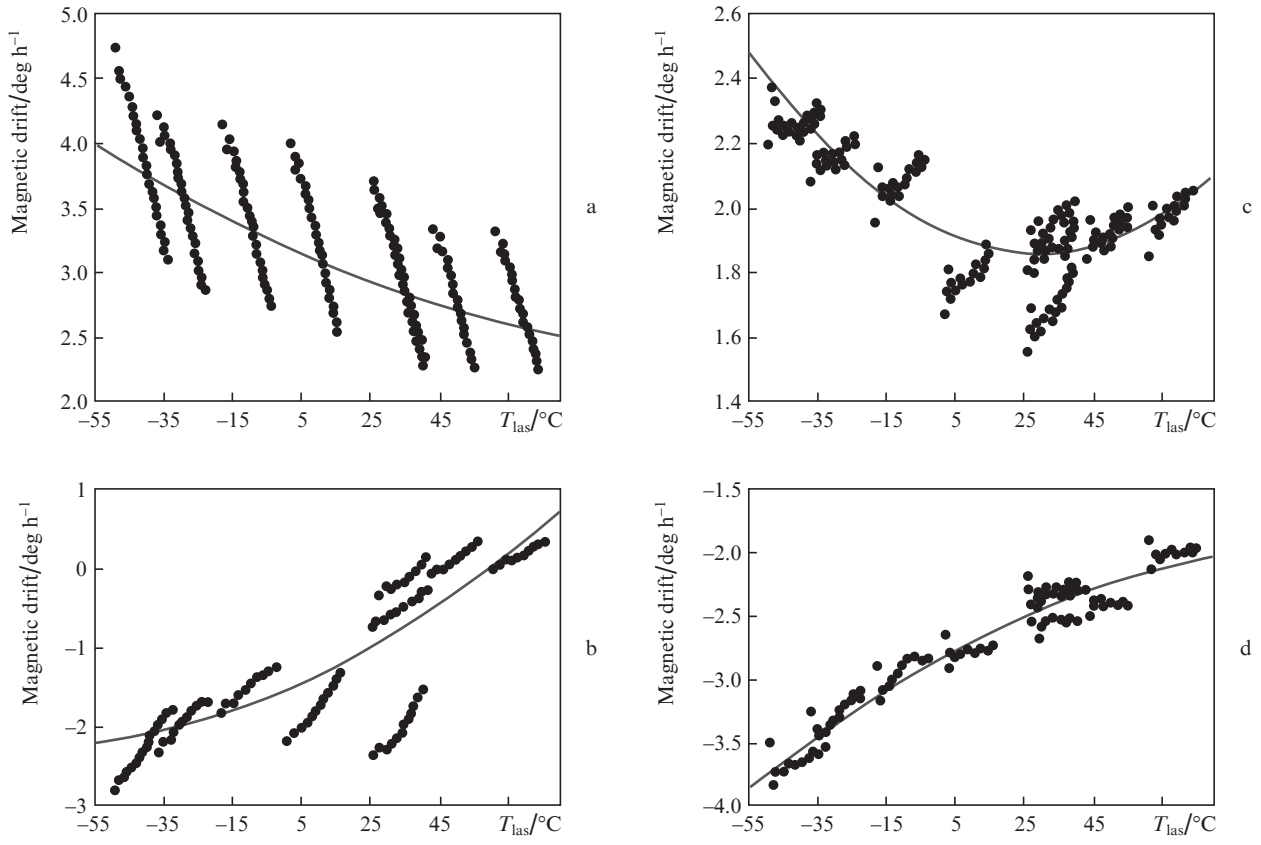

Figure 1. Typical dependences of the magnetic component of the drift in different ZLGs on the temperature (the lines plot the correcting functions in the form of the second-order polynomial with respect to T_{las}) in the cases when the dominant contribution is due to (a) the thermoelectric drift, (b) magnetoelastic drift and (c) thermoelectric and magnetoelastic drifts. In the case (d) the thermoelectric and magnetoelastic effects are insignificant, and only the temperature dependence of the magnetic sensitivity is expressed.

Institute') are presented in Fig. 2. The ZLG consists of the carrier construction, on which three Zeeman RLs (angular velocity sensors), functional electronics and a single- or double-layer shield are mounted. Each of the sensors also has its individual single-layer magnetic shield.

a

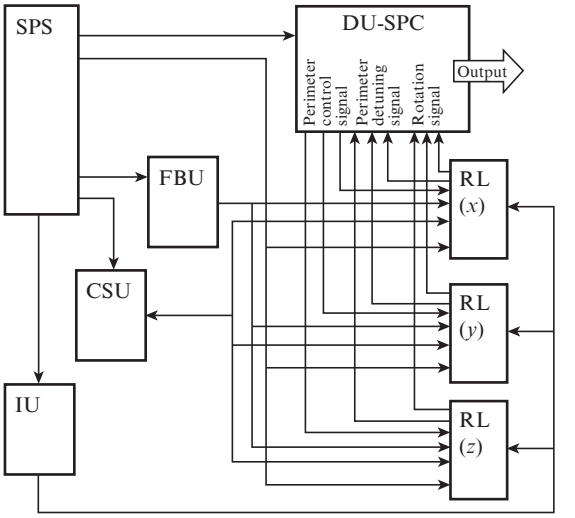

b

Figure 2. (a) External view and (b) structure schematic diagram of ZLG (see text):
(*1*) SPS; (*2*) RL; (*3*) FBU; (*4*) DU-SPC; (*5*) ZLG monitor.

The electronic equipment of the ZLG includes the following.

1. The current stabilisation unit and the board of photodetectors' supply (CSU-BPS), in which the stabilisation of gas discharge currents and supply voltages of photodetectors is implemented.

2. The frequency bias unit (FBU). In this unit the rectangular-shaped alternating current is generated that runs through the coils wound on gas discharge gaps of the RLs and induces a sign-alternating magnetic field in the active medium, which splits the frequencies of the counterpropagating waves.

3. The ignition unit (IU) generates high voltage at the moment of switching on the ZLG for inducing the initial breakdown in gas discharge gaps of the GLs, and then is switched off and does not affect further operation of the ZLG.

4. The digital unit and the system of perimeter control (DU-SPC) includes the digital reverse detector that transforms the sinusoidal beat signal of two counterpropagating waves into a sequence of pulses, and the system that automatically keeps the signal of the perimeter detuning to be zero [10].

5. The secondary power supply (SPS) that executes the DC-DC transformation of the electric voltages.

The ZLG has a hermetic carrier housing with a double-layer magnetic shield, enhancing the proof of the device against the external magnetic fields and the magnetic field of the SPS.

The power consumed by the ZLG is 27 W, and the maximal heat is released in the SPS (7 W) and the FBU (3.5 W). Therefore, the best way is to mount these units on the ZLG base having the thermal contact with the environment. Unfortunately, the attempts to develop an integrated SPS-FBU were not successful, because, as will be shown below, the magnetic component of the ZLG drift is very sensitive to the symmetry of the frequency biasing current, and even the minor perturbations from the SPS break this symmetry. For this reason the FBU is mounted on a separate board at the mutual crossbar carrying the ring lasers. Each of the RLs releases the power of 3.5 W, and all the rest units release 6 W. The heating of the RL during one hour of operation increases the temperature by 12 °C, the temperature of the crossbar (ZLG housing) being increased by 15.5 °C. These temperature increments are important for considering the magnetic drift due to the self-heating of the system.

4. Effect of external magnetic fields on the zero drift

In the Doppler limit ($\gamma_{ab}/ku \to 0$) in the maximum of the gain curve the linear approximation with respect to μ/ku yields the expression

$$f(0) = aH, \tag{5}$$

where the coefficient a determines the sensitivity of the ZLG to the magnetic field:

$$a = \frac{3.64}{\sqrt{\pi}} \frac{\lambda}{L} \frac{c}{u} G. \tag{6}$$

For typical values of the laser sensor parameters $a \approx 1.7$ kHz Oe^{-1}, which with the ZLG scale factor $M = 2.74$ deg (h Oe^{-1})$^{-1}$ yields the magnetic sensitivity ~4700 deg (h Oe^{-1})$^{-1}$. As follows from Eqn (6), the magnetic sensitivity is determined mainly by the gain. When the gain saturation is taken into account, for $G > p$ the important role is played by the losses p.

Due to the symmetric connection of gas discharge gaps in the laser sensors the sensitivity to the magnetic field is reduced by nearly 3.5 times. Its further decrease is implemented by using a multi-layer magnetic shield. A single-layer shield of the sensor reduces the sensitivity to less than 5 Hz Oe^{-1}, and the additional shielding of the triaxial ZLG provides a further reduction of the sensitivity by 100–500 times. In some cases it is reasonable to use four-layer shields, although the addition of new shields, as a rule, is limited by the mass and dimension requirements to the ZLG, and generally is not reasonable, because already with a three-layer shield the major role begins to be played by the instability of internal magnetic fields, as will be shown below. For the inner shield the most suitable material is the one having the maximal permeability and minimal magnetoelasticity, such as the 81NMA Permalloy. The outer shields of the ZLG operate in strong magnetic fields; therefore, for them both the permeability and the saturation induction are of importance. Among the available materials the 79NM Permalloy is the most suitable for external shields.

5. Effect of internal magnetic fields

In the presence of a stable internal magnetic field the variation in the magnetic component of the ZLG zero bias is caused by the change of its magnetic sensitivity under the temperature impact, similar to the case of the external magnetic fields. The resulting magnetic drift of the zero bias can be referred to as thermomagnetic drift.

The contribution to the internal magnetic field of the ZLG is caused mainly by the fields of magnetic parts inside the laser sensor or ZLG, the residual magnetic fields of the shields and the fields induced by the inner current sources. The magnetic elements inside the laser sensor should be eliminated, or their magnetisation should be reduced to the minimum; therefore, their effect is not considered in the present paper.

The residual magnetic field of the shields appears due to the magnetoelastic effects under the temperature and mechanical perturbations. The instability of the zero bias magnetic component in this case can be referred to as magnetoelastic drift.

The internal magnetic fields can be induced by the electric currents in the electronic functional systems, as well as by the currents, caused by the thermal electromotive force in the mounting construction. The methods for reducing the effect of the electronic circuits are well known, and so below we consider the effect of uncontrollable thermal electromotive forces, appearing at the junction of dissimilar materials, which can be referred to as sources of thermoelectric drift.

A special case is the influence of the current variations of the nonreciprocal device, generating the frequency bias, and the SPC voltage, providing the tuning of the cavity to the gain maximum, on the stability of the zero bias magnetic component. As shown below, since in this case the magnetic drift is caused by the changes, correlated with the bias switching frequency, this drift can be referred to as the dynamic magnetic drift.

5.1. Thermomagnetic drift

As follows from Eqns (5) and (6), the frequency difference between the counterpropagating waves, caused by the residual magnetic field H_{resid} in the active medium, in the first approximation is given by

$$f_{\text{m}} = 1.75 \times 10^5 \frac{\lambda}{L} \frac{G}{\sqrt{T_{\text{a}}}} H_{\text{resid}}, \tag{7}$$

where T_{a} is the temperature of the active medium.

As follows from Eqn (7), the stability of the ZLG magnetic sensitivity is determined, first of all, by the stability of the gain and temperature of the active medium, since the stability of the cavity length and the radiation wavelength is greater by many orders of magnitude. Although the active medium gain depends on many factors, it is efficiently controllable by the variation of the discharge current. Keeping the stability of the active medium temperature is much more difficult, that is why under the real conditions its variations due to both self-heating and to the changes in the external temperature become the dominant factor of the instability of the ZLG magnetic sensitivity. With the temperature variation the magnetic component will vary inversely proportional to T. The resulting drift of the zero can be referred to as the thermomagnetic drift f_{m}. At small changes in the temperature T_{a}, a simple expression for the relative value of the thermomagnetic drift follows from Eqn (7):

$$\frac{\Delta f_{\text{m}}}{f_{\text{m}}} = -\frac{1}{2} \frac{\Delta T_{\text{a}}}{T_{\text{a}}}. \tag{8}$$

The experimental dependence of the magnetic sensitivity on the RL temperature is presented in Fig. 3. One can see that in the entire range of operating temperatures the variation in the magnetic sensitivity does not exceed ±20%, in good agreement with the estimate given by Eqn (8). No hysteresis is observed.

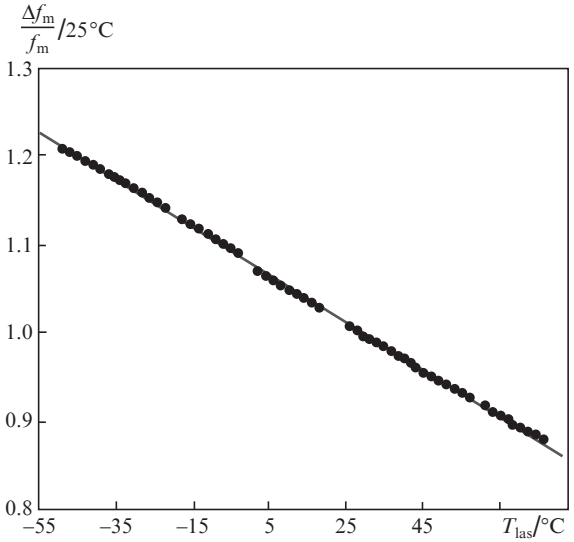

Figure 3. Dependence of the ZLG relative magnetic sensitivity on the temperature.

To approximate the dependence of the ZLG magnetic sensitivity on the temperature it is sufficient to use a linear function, the deviation from the approximated values not exceeding 0.5%. This fact means that for the typical ZLG magnetic zero bias of 10 deg h^{-1} the thermomagnetic drift will not exceed 0.05 deg h^{-1}.

5.2. Magnetoelastic drift of the ZLG

To protect the Zeeman RL from the external magnetic fields, it is placed in a multi-layer (commonly three- of four-layer) magnetic shield [11] made of a magnetically soft material with a large permeability coefficient and small, but nonzero, residual magnetisation [12]. After performing the technological operation of demagnetisation in an alternating magnetic field, the residual magnetisation does not exceed 0.005 Oe (which is by 100 times smaller than the magnetic field of the Earth). The magnetic sensitivity of the ZLG amounts to 2700–3000 deg (h $Oe^{-1})^{-1}$, i.e., the magnetic drift component can reach 15 deg h^{-1}. The change in the residual magnetisation under the temperature variations is caused by two magnetic effects, namely, the change in permeability [12] and the change in both the magnitude and the direction of the residual magnetisation of the inner shield due to its deformation (magnetoelastic effect) [13]. Note that this phenomenon demonstrates the temperature hysteresis, i.e., irreproducibility from one switching to another, which explains the appearance

of well-reproducible hysteresis of the magnetic drift temperature curve (see Figs 1a and 1d).

In order to reduce the magnetoelastic effects, for the RL magnetic shields one should use the material with the minimal magnetoelasticity, the 81NMA Permalloy, where the saturation magnetostriction amounts to 0.5×10^{-6}, which is by 4 times smaller than in the commonly used 79NM (2×10^{-6}) [12]. Besides, it is necessary to reduce the ZLG magnetic sensitivity by reducing the losses in the ZLG cavity and the active medium gain.

5.3. Thermoelectric drift of the ZLG

Consider a simplified scheme of the RL design (Fig. 4a). It has four junctions between different metals, where the thermal electromotive force can arise. The equivalent electric circuit is presented in Fig. 4b. It is seen that the current I runs in the housing and in the shields in the opposite directions.

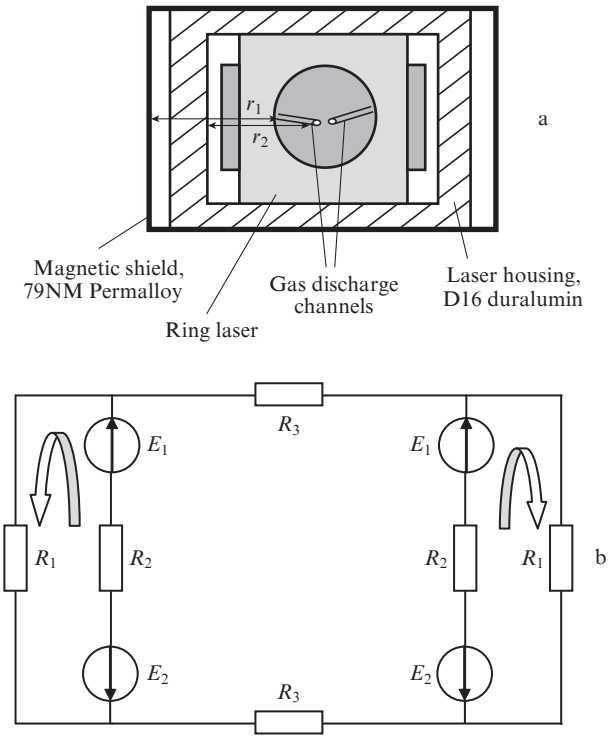

Figure 4. (a) Simplified construction scheme of the RL (the RL gas discharge channels are separated by the distance r_1 from the magnetic shield and by r_2 from the gyro housing) and (b) the equivalent electric circuit of the fastener assembly with the shield:
(E_1) thermal electromotive force of the junction 79NM-D16; (E_2) thermal electromotive force of the junction D16-79NM; (R_1) resistance of the magnetic shields, including the resistance of the junctions between the housing and the magnetic shields; (R_2) resistance of the laser housing; (R_3) resistance of the upper part of the laser housing.

The strength of this current is

$$I = \frac{E_1 - E_2}{R_1 + R_2 + 2R_{\text{con}}}, \tag{9}$$

where E_1 and E_2 are the thermal electromotive forces of the pair of materials of the screen and the shield at the junctions; R_1 is the resistance of the shield; R_2 is the resistance of the housing; and R_{con} is the contact resistance. The temperature difference T_1 between the upper part of the RL housing and its base leads to the difference of thermal electromotive forces

$$E_1 - E_2 = \alpha\Delta T_l, \tag{10}$$

where α is the coefficient of thermal electromotive force.

Due to the different distance from the active laser medium to the housing and to the magnetic shields, the magnetic field in the active medium appears to be nonzero,

$$H = \frac{\alpha\Delta T_l}{2\pi(R_1 + R_2 + 2R_{\text{con}})}\left(\frac{1}{r_2} - \frac{1}{r_1}\right). \tag{11}$$

In a real construction the contact resistance is large, $R_{\text{con}} \gg R_1, R_2$; therefore, it is just the one that determines the magnitude of the arising magnetic field. Taking into account also that $r_1 \gg r_2$, we obtain

$$H = \frac{\alpha\Delta T_l}{4\pi R_{\text{con}}}\frac{1}{r_2}. \tag{12}$$

The difference of temperatures ΔT_l that appears between the contacting pairs depends on the power P released in the laser and on the thermal resistance ρ of the carrying construction and the shield $\Delta T_l \approx P\rho$. The thermal resistance of the construction element is

$$\rho = \frac{l}{\lambda S}, \tag{13}$$

where l is the length of the element; λ is the thermal conductivity coefficient; and S is the cross-section area of the element.

If the electric resistances of the shield and the carrying construction are connected in sequence, then their thermal resistances ρ_1 and ρ_2 are connected parallel, so that

$$\rho = \left(\frac{1}{\rho_1} + \frac{1}{\rho_2}\right)^{-1} = \frac{\rho_1\rho_2}{\rho_1 + \rho_2}. \tag{14}$$

Thus, the arising magnetic field, directed along the laser channel is

$$H = \frac{\alpha Pl}{4\pi r_2 R_{\text{con}}\lambda_2 S_2}\left(1 + \frac{\lambda_1 S_1}{\lambda_2 S_2}\right)^{-1}. \tag{15}$$

Since the construction geometry and the shield material are given, consider the arising magnetic field by the example of two materials of the carrying construction, the titanium and aluminium alloys. In the case of the titanium alloy and the 79NM Permalloy shield ($\alpha \approx 40$ μV K^{-1}, $\lambda_1 = 13$ W m^{-1} K^{-1}, $\lambda_2 = 9$ W m^{-1} K^{-1}) for the typical parameters of the sensors ($P \approx 0.5$ W, $R_{\text{con}} \approx 0.2$ Ω, $r_2 \approx 5$ mm, $S_1 \approx 130$ mm^2, $S_2 \approx 200$ mm^2) the estimate yields $H \approx 570$ μOe. In the case of the aluminium alloy the estimate is $H \approx 60$ μOe.

For the magnetic sensitivity $\alpha \approx 4700$ deg (h Oe^{-1})$^{-1}$ of the sensor to the magnetic field directed along the axis of the gas discharge channel of the laser, the estimate of the magnetic drift is ~2.7 deg h^{-1} for the titanium alloy and 0.28 deg h^{-1} for the aluminium alloy, i.e., the use of aluminium alloys for

the carrying construction of the ZLG is preferable. It is worth noting that if the carrying construction is made of different materials, e.g., the columns are made of titanium and the base with the clamping of aluminium, then the temperature gradient between the different columns will give rise to a similar effect even in the absence of contact with the shields.

This phenomenon manifests itself in the fast variation of the magnetic drift in the process of the self-heating of the device, the resulting change being nearly the same at different temperatures (see Fig. 1a). The efficient method for suppressing this effect is the deposition of a non-conducting film on the parts of the housing that blocks the electric current. The experimental confirmation is presented in Fig. 5.

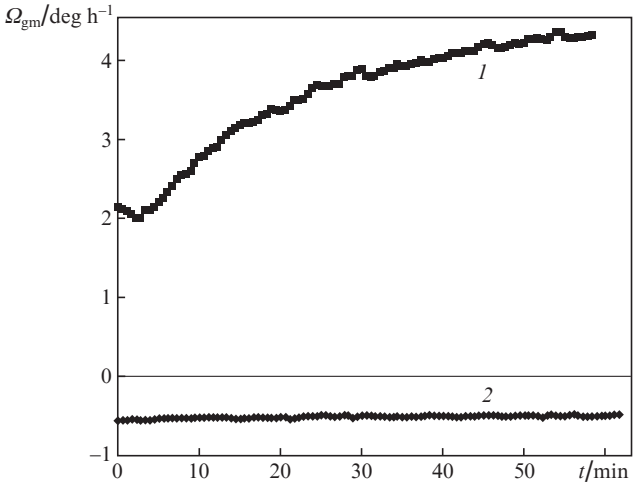

Figure 5. Dependences of the ZLG magnetic drift on its operation time t for the cases when the parts of the RL are not electrically isolated (*1*) and are electrically isolated (*2*).

5.4. Dynamic magnetic drift

The dynamic magnetic drift is mainly due to the operation of the FBU. The output current of the FBU runs through the blocking capacitor, thus supporting the equality of the integrals of the bias current in half-periods (the direct current is equal to zero). However, the amplitudes of the bias current in half-periods and the durations of half-periods can be different, since the electronic circuit keeps constant only the mean amplitude of the bias current. In this case the nonlinearity of the dependence of the frequency difference between the counterpropagating waves on the magnetic field leads to the dynamic drift.

Indeed, expanding expression (1) in power series with respect to the ratio μ/ku up to the third order, we obtain

$$f = aH + bH^3, \tag{16}$$

where $b = -2\mu_B^2 a/3(ku)^2$.

The frequency bias unit operates with the zero constant component of the current, and, therefore, the constant component of the magnetic field strength H will be zero, too. This fact means that the magnetic fields during the positive (H^+) and negative (H^-) half-periods of the current are related as

$$H^+\frac{\tau+\Delta\tau}{2} = H^-\frac{\tau-\Delta\tau}{2}, \tag{17}$$

where τ is the mean duration of the bias commutation half-period, and $\Delta\tau$ is the difference of durations of the positive and negative half-periods.

From Eqn (1) one can derive the expression for the magnetic drift of the frequency difference due to the bias asymmetry Δf_{gmd}:

$$\Delta f_{gmd} = M\Big(f^+\frac{\tau+\Delta\tau}{2} - \frac{\tau-\Delta\tau}{2}f^-\Big)\tau^{-1} \approx -MbH^3\frac{\Delta\tau}{\tau}, \tag{18}$$

where H is the mean amplitude value of the magnetic field, induced by the FBU current during the bias commutation period; and f^+ and f^- are the beating frequencies for the counterpropagating waves during the positive and negative half-periods of the bias current. For the magnetic field strength 40 Oe, $\Delta\tau/\tau = 10^{-3}$, and $T = 25\,^\circ$C we obtain $\Delta f_{gmd} = 0.06$ deg h^{-1}.

The dynamic drift caused by the variations in the frequency bias, synchronous with the bias commutation, has similar character.

The dynamic drift can be also caused by the parasitic currents induced in the SPC circuits by the FBU and SPS currents.

Since the time constant of the SPC is chosen to be much smaller than τ, the pulsations are easily transmitted by the SPC voltage circuit to the piezoengines, causing the harmonic oscillations of the cavity perimeter:

$$\Delta\lambda = \frac{\Delta U\sin(2\pi\nu t + \phi_0)}{U_\lambda}, \tag{19}$$

where U_λ is the voltage, corresponding to the change in the cavity perimeter of the RL by one wavelength; ΔU is the SPC circuit voltage pulsation amplitude; ν is the SPC circuit voltage pulsation frequency; and ϕ_0 is the initial phase of the pulsations.

Then, using Eqn (5), the value of the drift $\Delta\Omega_{gms}$, caused by the SPC pulsations in the absence of the static cavity detuning can be expressed as

$$\Delta\Omega_{gms} = -M\frac{f_0\chi_0}{\tau}\left(\frac{\Delta U}{U_\lambda}\right)^2\frac{1}{2\pi\nu}\sin(2\pi\nu\tau + 2\phi_0)\sin^2(\pi\nu\tau). \tag{20}$$

Obviously, the dynamic drift decreases with increasing pulsation frequency, i.e., the frequency of the secondary power supply convertor. For the pulsation frequency being a multiple of the bias commutation frequency the drift is equal to zero. For the pulsation frequency being a multiple of the half of the bias commutation frequency,

$$\Delta\Omega'_{gms} = \pm M\frac{2f_0\chi_0}{m\pi}\left(\frac{\Delta U}{U_\lambda}\right)^2\sin(2\phi_0), \tag{21}$$

where m is the number, equal to the ratio of the pulsation frequency and the bias commutation frequency. Note that for ϕ_0 equal to zero or being a multiple of $\pi/2$, the drift is also equal to zero.

The presence of the static detuning of the RL perimeter essentially changes the situation. In this case the additive term appears

$$\Delta\Omega''_{gms} = M\frac{2f_0\chi_0}{\pi\nu\tau}\frac{\Delta U}{U_\lambda}\frac{\Delta U_0}{U_\lambda}\sin(2\pi\nu\tau + 2\phi_0)\sin^2(\pi\nu\tau/2), \tag{22}$$

that determines the drift induced by the crosstalk at the pulsation frequencies being a multiple of the bias commutation frequency. For the pulsation frequency being a multiple of odd harmonics of the bias commutation frequency

$$\Delta\Omega''_{\text{gms}} = M\frac{4f_0\chi_0}{(2m+1)\pi}\frac{\Delta U}{U_\lambda}\frac{\Delta U_0}{U_\lambda}\sin[(2m+1)\pi+\phi_0]. \quad (23)$$

Note that for $\phi_0 = \pi + 2m\pi$ the drift is also equal to zero.

Let us estimate the contribution of the dynamic drift due to the pulsations of the voltage at the piezoceramics induced by the SPS in the absence of detuning. For $m = 200$, $f_0 = 50$ kHz, $\Delta U/U_\lambda = 0.002$ and $\chi = 5$ we obtain $\Delta\Omega_{\text{gms}} = 0.01$ deg h^{-1}.

In the presence of detuning, the crosstalk from the FBU at the switching frequency and its odd harmonics become dominant. Let us estimate the contribution of the first harmonic. For $\Delta U/U_\lambda = 0.002$ we obtain $\Delta\Omega_{\text{gms}} = 3.6$ deg h^{-1}.

Thus, the most important method for suppressing the dynamic drift is the reduction of the static detuning, which is achieved both by the increasing the amplitude of the useful signal from the SPC photodetector and by shielding all circuits, including the piezoengines, from the crosstalk induced by the FBU current.

6. Algorithmic correction of reproducible magnetic drifts

The typical temperature dependences of the drift magnetic component for the RL K-5, presented in Fig. 1, were obtained in the triaxial ZLG operating in the regime of switching the modes having orthogonal polarisations with the interval between the switchings 60 s and the operation time 1 h, at the constant temperature and fixed position of the device with respect to the Earth surface. The analysis of the presented dependences shows the following.

1. The absolute value of the zero bias magnetic component does not exceed 8 deg h^{-1}.

2. During a single switching of the system the magnetic drift due to the self-heating (15 °C h^{-1}) achieves 1.6 deg h^{-1}. As a rule, no correlation is observed between the changes of the magnetic drift in the three RLs of one ZLG, which evidences in favour of the absence of dynamic drifts, related to the electronic units. The change in the magnetic drift is weakly dependent on the temperature of the RL. In all four cases a linear dependence of the magnetic drift change on the change in the temperature is observed within a given switching of the system.

3. The typical irreproducibility of the magnetic drift (the difference between the values at the same temperature in different switchings of the system) amounts to 0.3 deg h^{-1}, and only in some RLs it can achieve 1.5 deg h^{-1} (Fig. 1c). Conclusions 1 and 2 remain true for such a ZLG.

From the analysis it becomes clear that the cause of the instability of the zero bias magnetic component (drift) within a single switching on of the ZLG is the thermoelectric drift, and the cause of its irreproducibility is the magnetoelastic drift.

To compensate for the reproducible dependences of the magnetic drift one can use a correcting function, approximating the drift. The simplest correcting function is a polynomial of the first or of the second order, in which the role of the argument is played by the RL temperature T_{las}. However, as seen from Fig. 1, only for the realisations shown in Fig. 1d this function provides a good approximation of the magnetic drift, and an increase in the polynomial power does not provide essential improvement. It is required to choose a more optimal method of the magnetic drift correction.

In our opinion, the form of the correcting function depends on the sequence diagram of the ZLG use. Two cases should be distinguished here.

1. At the moment of switching on, the ZLG does not move with respect to the Earth surface. Here one can measure the initial values of the magnetic drift Ω_{gm0} at the moment of switching on and then execute the further correction by the difference of the RL temperature T_{las} from its initial value T_{las0} at the moment of switching on. As seen from Fig.1, the magnetic drift is well described by the linear function of the change in the laser temperature T_{las} with respect to T_{las0}, and is calculated using the expression:

$$\Omega_{\text{gm}} = \Omega_{\text{gm0}} + A_{\text{gm}}(T_{\text{las}} - T_{\text{las0}}). \quad (24)$$

The temperature coefficient of the magnetic drift A_{gm}, depending on T_{las0}, is measured in advance, during the fabrication of the ZLG (Fig. 6a).

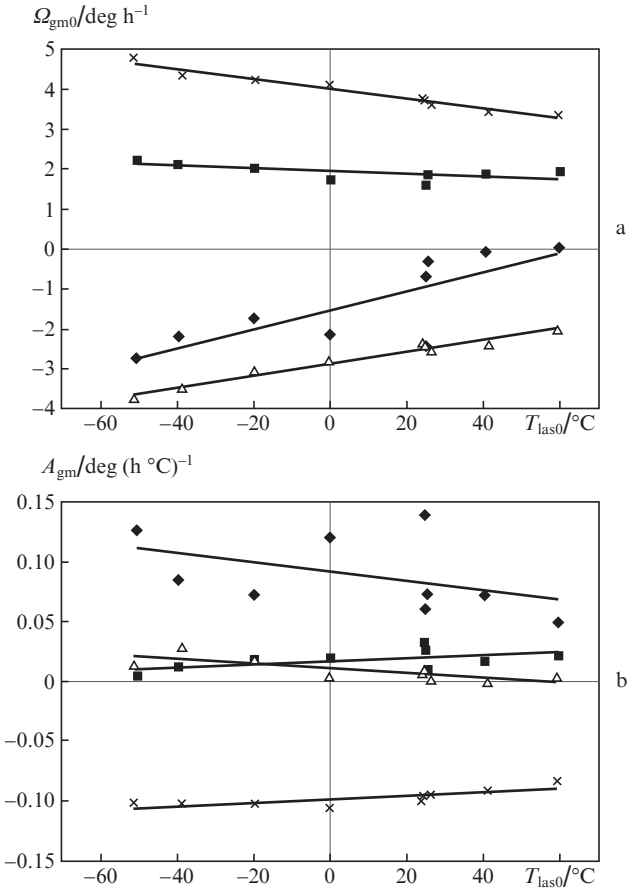

Figure 6. Dependence of the coefficients (a) Ω_{gm0} and (b) A_{gm} on the RL temperature for the magnetic drifts, presented in Fig. 1a (×), 1b (◆), 1c (■) and 1d (△). The lines plot the result of calculations performed using Eqns (24) and (25).

2. At the moment of switching on, the device moves with respect to the Earth, i.e., the selection of the initial value Ω_{gm0} is impossible. In this case the dependence of Ω_{gm0} on T_{las0} is measured in advance, during the fabrication of the ZLG (Fig. 6b):

$$\Omega_{gm0}(T_{las0}) = C_{gm0} + B_{m0}(T_{las0} - T_0), \quad (25)$$

where T_0 is the 'normal climatic temperature', commonly assumed to equal 25 °C.

Unfortunately, the use of Eqn (25) becomes problematic if the device was heated before the beginning of the measurement, particularly in the case, when the heated device was switched off and then after some time switched on again. If the temperature of the environment is known, it may be taken for T_{las0}, but usually the installation of thermal sensors on the outside of the ZLG is not possible. In this case the thermal sensor should be installed on the ZLG housing, and the difference between the temperature of the housing and the temperature of the RL should be measured (Fig. 7). As seen from Fig. 7, the dependences of the temperatures of RL T_{las} and the housing T_h on the operation time t is described by the formulae:

$$T_{las} = A_T(1 - \exp(-1/\tau_T)) + A_{Th}(1 - \exp(-1/\tau_{Tc})) + T_{las0},$$
$$T_h = A_{Th}(1 - \exp(-1/\tau_{Th})) + T_{las0}. \quad (26)$$

The coefficients A_T, A_{Th}, τ_T and τ_{Th} are determined during the factory adjustment.

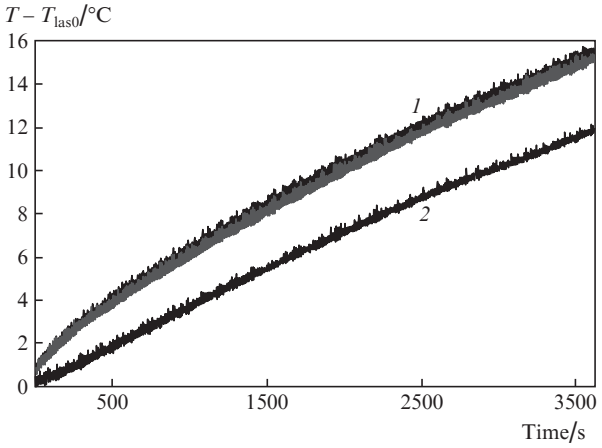

Figure 7. Variation in the temperature of (*1*) three RLs and (*2*) the ZLG housing in the course of self-heating.

Then from Eqn (26) it is possible to find the moment t of the beginning of information reception for the present switching on and T_{las0}:

$$t = -\ln\left(1 - \frac{T_{las} - T_h}{A_T}\right)\tau_T,$$
$$T_{las0} = T_h - A_{Th}(1 - \exp(-1/\tau_{Th})). \quad (27)$$

Then Ω_{gm0} is calculated using Eqn (25) and Ω_{gm} using Eqn (24).

The results of using the present calculation algorithm and the correcting function are shown in Fig. 8. It is seen that the reduction of the magnetic drift almost to the Ω_{gm0} reproducibility (0.22–0.35 deg h^{-1}) appears to be possible in the cases shown in Figs 1a–c, and to 0.9–1.5 deg h^{-1} in the case of Fig. 1d.

The summary results of the Ω_{gm} calculations before and after the application of the algorithmic correction for different versions of using the RL K-5 are the following: if during the

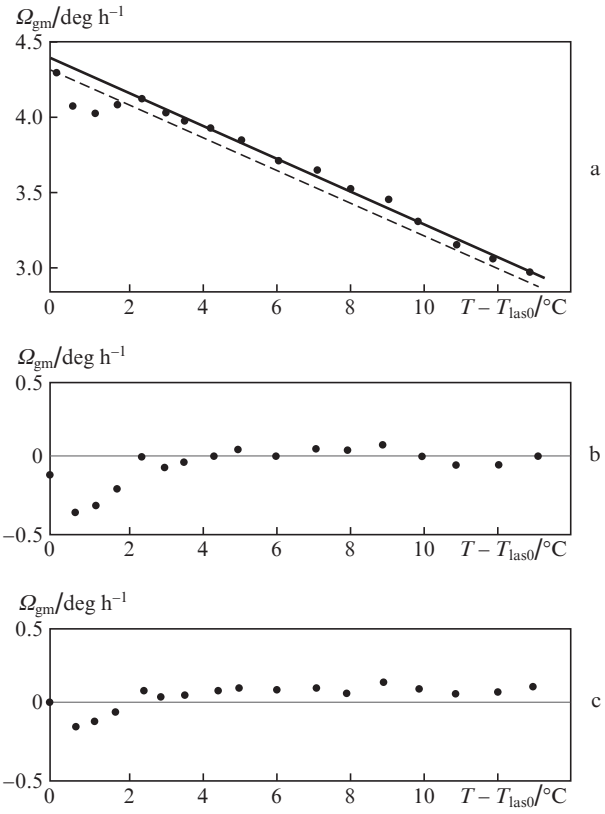

Figure 8. Residual errors of approximation of the ZLG drift magnetic component. Dependence of the drift magnetic component on the temperature due to self-heating (the solid line plots the correcting function without the initial calibration of Ω_{gm0}, the dashed line – with the initial calibration of Ω_{gm0}) (a), the residual magnetic drift after the correction without the Ω_{gm0} initial calibration (b), and the residual drift after correction with the Ω_{gm0} initial calibration (c).

switching on the device changes its orientation with respect to the Earth, then the magnetic drift amounts to 0.6–2.5 deg h^{-1} before the correction and to 0.35–1.4 deg h^{-1} after the correction, and if the device is motionless during the switching on, then 0.35–1.6 deg h^{-1} and 0.22–0.9 deg h^{-1}, respectively. The results are obtained for the continuous operation time 1 h and the time interval 60 s between the mode switching.

7. Conclusions

Provided that the shielding is sufficient, the external magnetic field is not dominant in the formation of the magnetic component of the ZLG zero bias, and the latter is mainly caused by the internal magnetic fields, its instability being determined by the sum of the thermomagnetic, magnetoelastic and dynamic magnetic drifts. Except the thermomagnetic drift, easily approximated by the temperature dependence, each of the drifts is significant and contributes to the error. However, it appeared possible to develop the methods that reduce their magnitude by 4–10 times. For the magnetoelastic drift it is the use of materials with low magnetostriction (81NMA Permalloy), while for the thermoelectric drift it is the use of homogeneous materials (first of all, D16) and electrically isolating coating of parts. In the case of the dynamic drift it is of major importance to reduce the static and dynamic detuning, which is achieved by increasing the amplitude of the useful signal from the SPC photodetector and by shielding all cir-

cuits, including the piezoengines, from the crosstalk induced by the FBU current.

The use of algorithmic correction allows the reduction of the magnetic drift by 2 times.

The measures listed above allow the magnetic drift of the ZLG to be no greater than 0.15 deg h^{-1} in the case of a motionless device and 0.3 deg h^{-1} for a moving device. For the ZLG operating in the quasi-four-wave regime this increases the total drift by only 0.0025 and 0.005 deg h^{-1}, respectively.

References

1. Dmitriev V.G., Golyaev Yu.D., Vinokurov Yu.A., Kolbas Yu.Yu., Tikhmenev N.V. *Materialy 15-y Mezhdunarodnoy konferentsii po integrirovannym navigatsionnym sistemam* (Proc. 15 Int. Conf. 'Integrated Navigation Systems') (S.-Petersburg: TsNII Elektropribor, 2008) p. 127.
2. Golyaev Yu.D., Dmitriev V.G., Kazakov A.A., Kolbas Yu.Yu., Nazarenko M.M., Tikhmenev N.V., Yakushev A.B. Patent of Russian Federation No. 2408844, the priority of 07.10.2009.
3. Vinokurov Yu.A., Golyaev Yu.D., Dmitriev V.G., Kazakov A.A., Kolbas Yu.Yu., Tikhmenev N.V., Yakushev A.I. Patent of Russian Federation No. 2418266, the priority of 11.01.2010.
4. Vakhitov N.G., Golyaev Yu.D., Dronov I.V., Ivanov M.F., Kolbas Yu.Yu., Krutikov A.P. *Vestn. Mosk. Gos. Tekh. Univ. im. N.E. Baumana, Ser. Priborostroen.*, **3** (90), 112 (2013).
5. Golyaev Yu.D., Dronov I.V., Kolbas Yu.Yu., Pryadein V.A., Shpikalov B.N. *Vestn. Mosk. Gos. Tekh. Univ. im. N.E. Baumana, Ser. Priborostroen.*, **3** (88), 112 (2012).
6. Golyaev Yu.D., Ivanov M.A., Kolbas Yu.Yu., Krutikov A.P., Aristarkhova M.A., Belov A.V., Solovyova T.I. *Setevoi Elektronnyi Nauchn. Zh. 'Sistemotekhnika'*, (10), 48 (2012).
7. Golyaev Yu.D., Kolbas Yu.Yu. *Zh. Tekh. Fiz.*, **17**, 162 (1991).
8. Golyaev Yu.D., Kolbas Yu.Yu. *Kvantovaya Elektron.*, **42**, 949 (2012) [*Quantum Electron.*, **42**, 949 (2012)].
9. Savelyev I.I., Khromykh A.M., Yakushev A.I. *Kvantovaya Elektron.*, **6**, 1155 (1979) [*Sov. J. Quantum Electron.*, **9**, 682 (1979)].
10. Golyaev Yu.D., Mel'nikov A.V., Solovyov Yu.N., Telegin G.I., Yaremenko S.O. *Elektron. Tekh., Ser. 11. Lazer Tekh. Optoelektron.*, No. 1 (57), 62 (1991).
11. Golyaev Yu.D., Kolbas Yu.Yu. *Elektron. Tekh., Ser. 11. Lazer Tekh. Optoelektron.*, No. 2 (58), 76 (1991).
12. *Splavy pretsizionnye magnitno-myagkiye. Tekhnicheskiye usloviya. GOST 10160-75* (High-Precision Magnetically Soft Alloys. Technical Requirements. The State All-Union Standard 10160 (Moscow: Gosstandart, 1975).
13. Bakharev M.S. *Doct. Diss.* (Tomsk: Tomsk Polytechnic University, 2004).